

ORIGINAL RESEARCH ARTICLE

Sustainable amorphous porous carbon for efficient removal of industrial dyes

Supplementary Files

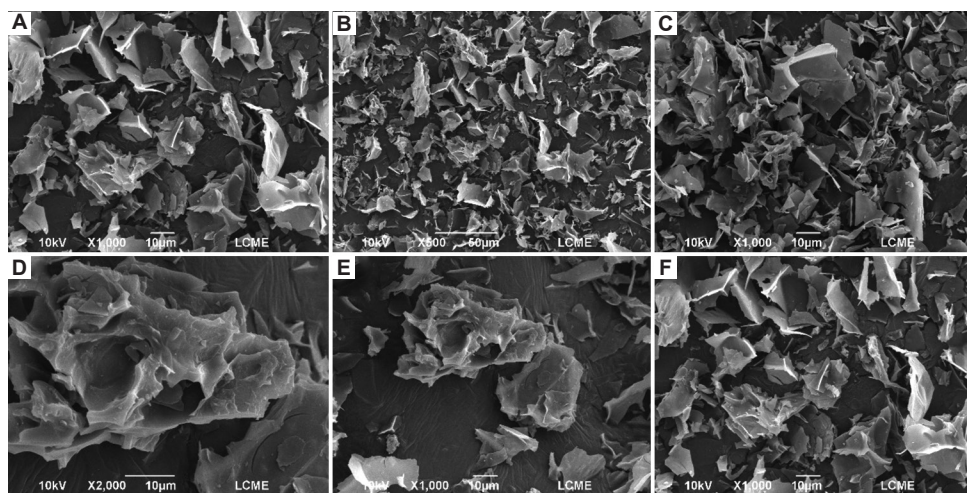


Figure S1. Scanning electron microscopy images of cork-derived activated carbon. Scale bars: (A, C, D, E, F) 10 µm, (B) 50 µm; magnification: (A, C, E, F) ×1,000, (B) ×500, (D) ×2,000.

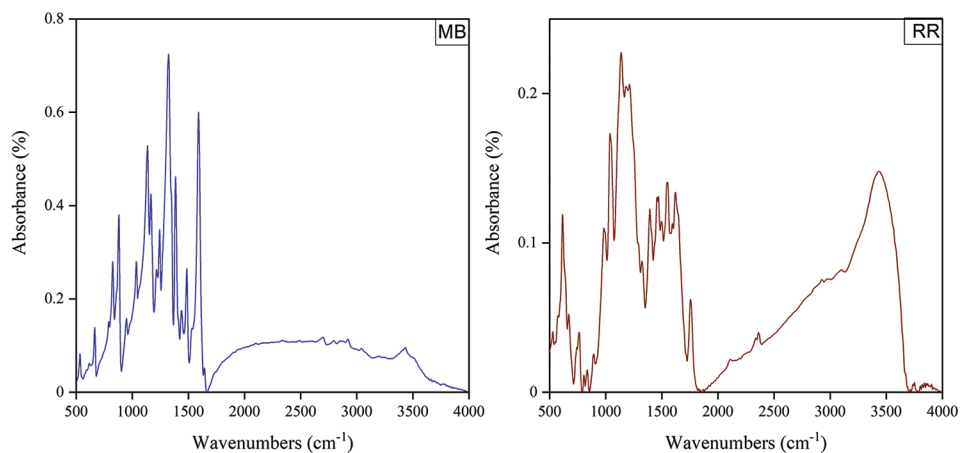


Figure S2. Fourier transform infrared spectra of methylene blue (MB) and reactive red (RR) dyes

Table S1. Equations utilized in this study

Adsorption model	Equation	Parameters	References
Kinetic model equations			
Pseudo-1 st -order kinetic	$q_t = q_e(1 - e^{-k_1 t})$	k_1 (min ⁻¹) rate constants; q_t , q_e , and q_{AV} =theoretical values for the adsorption capacity.	1
Pseudo-2 nd -order kinetic	$q_t = \frac{t}{\left(\frac{1}{k_2 q_2^2}\right) + \left(\frac{t}{q_2}\right)}$	q_t , q_e , and q_{AV} =theoretical values for the adsorption capacity, k_2 (g-mg-min ⁻¹) are the rate constant (mg-g ⁻¹).	2
Intraparticle diffusion	$q_t = K_{diff} t^{1/2} + C$	q_t (mg-g ⁻¹) is the adsorption capacity at a given time, t (min) is the time of the adsorption process studied, k_{diff} is the intraparticle diffusion rate constant (g-mg/min), and C (mg/g) is a constant related to the diffusion resistance and the thickness of the boundary layer.	3
Elovich	$q_t = \frac{\ln(\alpha\beta)}{\beta} + \frac{1}{\beta} \ln t$	α (mg g/min) is the initial adsorption rate, β (g/mg) is related to the extent of surface coverage and activated energy in the chemisorption process, (mg/g) is the amount adsorbed in a time t (min), and the intercept of q_t versus $\ln t$ corresponds to the amount adsorbed during the initial phase of adsorption.	4
Isotherm model equations			
Langmuir	$q_e = q_L \frac{K_L C_e}{1 + K_L C_e}$	q_L =maximum adsorption capacity of the Langmuir model (mg-g ⁻¹); K_L =Langmuir constant (L/mg ⁻¹).	5
Freundlich	$q_e = K_f C_e^{1/n}$	K_F =Freundlich constant (mg-g ⁻¹) (mg-L ⁻¹) ^{-1/nF} , $1/n$ =heterogeneity factor.	6
Redlich-Peterson (R-P)	$N = \frac{KC}{(1 + \alpha C^n)}$	N is the amount adsorbed at equilibrium; K is the R-P constant; C is the equilibrium concentration; α is R-P parameter, and n is the exponential factor.	7
Equations thermodynamic parameters			
Thermodynamics model	$\Delta G^0 = -RT \ln(K_e)$ $\Delta G^0 = -RT \ln(K_e)$ $\Delta G^0 = \Delta H^0 - T \Delta S^0$ $k_e = \frac{k M_W \gamma^D}{\gamma}$	k_e =equilibrium constant; k =constant parameter from the most suitable isotherm fit (L-mg ⁻¹); M_W =molecular weight of the dyes (g-mol ⁻¹); γ^D =activity coefficient of dyes in solution (dimensionless, assuming $\gamma = 1$); γ = unitary activity coefficient of MB (1 mol-L ⁻¹); T =temperature (K); R =universal gas constant (8.31×10 ⁻³ kJ-mol ⁻¹ .K ⁻¹).	8
Column equation models			
Clark	$\frac{C_t}{C_i} = \frac{1}{[1 + A e^{-rt}]^{n-1}}$	n is the Freundlich constant; r is the Clark or fractal-like Clark constant (min ⁻¹); A is the Clark constant.	9
Thomas	$\frac{C_t}{C_i} = \frac{1}{1 + e^{-\frac{K_{Th}}{Q} (q_i^x - C_0 V_{eff})}}$	K_{Th} is the Thomas model constant (mL-min-mg ⁻¹); V_{eff} is the effluent volume (mL).	10
Yoon-Nelson	$\frac{C_t}{C_i} = \frac{1}{1 + e^{K_{YN}(\tau - t)}}$	K_{YN} is the rate constant (1/min); τ , the time required for 50% adsorbate breakthrough (min); and t is the breakthrough (sampling) time (min).	11

Table S2. Structural parameters of cork-derived activated carbon produced by chemical activation with potassium hydroxide (KOH) under different experimental conditions

Material	Activation type	KOH quantity	Temperature (°C)	SSA _{BET} (m ² ·g ⁻¹)	V _{mic} (cm ³ ·g ⁻¹)	References
Cork	KOH	0.25 g	500	354	0.15	12
		0.5 g		427	0.18	
		1 g		507	0.21	
		0.25 g	600	498	0.21	
		0.5 g		561	0.24	
		1 g		723	0.30	
		0.25 g	700	73	0.34	
		0.5 g		1,050	0.45	
		1 g		106	0.45	
		0.25 g	800	1,044	0.43	
		0.5 g		1,190	0.51	
		1 g		1,336	0.56	
		Cork	KOH	1:1 ^a	700	
1:1 ^a	800			948	0.41	
1:2 ^a	700			874	0.38	

Note: ^aMass ratio between activated carbon and KOH.

Table S3. Kinetic parameters for the adsorption of methylene blue (MB) and reactive red (RR) dyes

Parameter	MB	RR
Pseudo-first-order		
q _e (mg/g)	249.96±0.02	97.17±1.23
K ₁ (min ⁻¹)	5.98±0.11	0.20±0.01
R ²	0.9935±0.005	0.9936±8.15
Pseudo-second-order		
q _e (mg/g)	250.05±0.01	102.86±0.67
K ₁ (g·mg/min)	1.54±0.12	0.01±2.08
R ²	0.9985±0.002	0.9987±1.56
Elovich		
B (mg/g)	0.407±0.09	0.10±0.01
R ²	0.9977±16.25	0.9837±22.37

Table S4. Parameters of isotherms for the adsorption of methylene blue (MB) and reactive red (RR) dyes

Parameter	MB	RR
Langmuir		
q _m (mg/g)	607.89±28.27	252.40±56.79
B (L/mg)	2.42±0.51	0.08±0.06
R ²	0.9857±0.81	0.8454±0.79
Freundlich		
K _F	359.89±22.52	49.04±0.73
n	0.26±0.03	0.37±0.004
R ²	0.9658±0.75	0.9998±0.71
Redlich-Peterson		
q _m (mg/g)	3517.47±3.34	457.36±3.56
α (L/mg)	7.88±4.17	8.83±3.12
β (L/mg)	0.84±0.04	0.63±0.95
R ²	0.9941±0.52	0.8562±0.72

Table S5. Thermodynamics parameters for the methylene blue (MB) and reactive red (RR) dyes

Dye	Temperature (K)	kc	ΔG (kJ/mol)	ΔH (kJ/mol)	ΔS (J/mol/K)
MB	298	8.251×10^2	-1.25×10^4	75.456	56.092
	308	8.272×10^2	-1.31×10^4		
	318	8.276×10^2	-1.36×10^4		
	328	8.275×10^2	-1.42×10^4		
RR	298	14.681	9.067×10^5	-11.96×10^4	-45.601
	308	6.079	9.071×10^5		
	318	5.971	9.076×10^5		
	328	6.760	9.081×10^5		

Table S6. Parameters of the Thomas, Yoon-Nelson, and Clark kinetic models of adsorption in a fixed-bed column for the methylene blue (MB) and reactive red (RR) dyes

Model	Parameter	MB	RR
Thomas	K_{th} (mg/g)	0.0083 ± 0.002	0.0072 ± 0.001
	Q_0 (mg/g)	1992.07 ± 1.19	4500.48 ± 6.66
	R^2	0.9916 ± 0.001	0.9963 ± 0.007
Yoon-Nelson	K_{yn} (min ⁻¹)	0.03 ± 0.01	0.0413 ± 0.02
	R^2	0.9843 ± 0.002	0.9941 ± 0.001
	τ (h)	0.51 ± 0.42	0.44 ± 0.34
Clark	A (L/mg)	$1.9313 \times 10^7 \pm 2.70$	91814.5 ± 5.12
	r	0.0176 ± 0.001	0.01723 ± 0.08
	R^2	0.9852 ± 0.002	0.9950 ± 0.001

Table S7. Dye adsorption capacity of activated carbons

Precursor	SSA (m ² /g)	Dye	Adsorption capacity (mg/g)	References
Almond shells	1,133	Methylene Blue	788	14
Mangosteen peel	1,621	Methylene Blue	1,193	15
Rice husk	752	Methylene Blue	362.60	16
Seaweed	683	Reactive Red 23	59.88	17
		Reactive Blue 171	71.94	
		Reactive Blue 4	131.93	
Sewage sludge	159	Remazol Brilliant Blue R	33.07	18
Cork	1,793	Methylene Blue	250	This work
		Reactive Red	105	

References

- Lagergren S. About the theory of so-called adsorption of soluble substances. *K Sven Vetenskapsakad Handlingar*. 1898;24:1-39.
- Ho YS, McKay G. Sorption of dye from aqueous solution by peat. *Chem Eng J*. 1998;70:115-124. doi: 10.1016/S0923-0467(98)00076-1
- Weber WJ, Morris JC. Kinetics of adsorption on carbon from solution. *J Sanit Eng Div*. 1963;89:31-59.
- Ferreira AS, Mota AA, Oliveira AM, et al. Equilibrium and kinetic modelling of adsorption: Evaluating the performance of adsorbent in softening water for irrigation and animal consumption. *Rev Virtual Quim*. 2019;11:1752-1766. doi: 10.21577/1984-6835.20190123
- Langmuir I. The adsorption of gases on plane surfaces of glass, mica and platinum. *J Am Chem Soc*. 1918;40:136-1403. doi: 10.1021/ja02242a004
- Freundlich H. Über die adsorption in lösungen. *Zeitschrift Phys Chem*. 1907;57U:385-470. doi: 10.1515/zpch-1907-5723
- Ayawei N, Ebelegi AN, Wankasi D. Modelling and interpretation of adsorption isotherms. *J Chem*. 2017;2017:3039817. doi: 10.1155/2017/3039817
- Lima EC, Hosseini-Bandegharai A, Moreno-Piraján JC, Anastopoulos I. A critical review of the estimation of the thermodynamic parameters on adsorption equilibria. Wrong use of equilibrium constant in the Van't Hoof equation for calculation of thermodynamic parameters of adsorption. *J Mol Liq*. 2019;273:425-434. doi: 10.1016/j.molliq.2018.10.048
- Hu Q, Li H, Zhang Z, Pei X. Development of fractal-like clark model in a fixed-bed column. *Sep Purif Technol*. 2020;25:117396. doi: 10.1016/j.seppur.2020.117396
- Chen S, Yue Q, Gao B, Li Q, Xu X, Fu K. Adsorption of hexavalent chromium from aqueous solution by modified corn stalk: A fixed-bed column study. *Bioresour Technol*. 2012;113:114-120. doi: 10.1016/j.biortech.2011.11.110
- Omitola OB, Abonyi MN, Akpomie KG, Dawodu FA. Adams-Bohart, Yoon-Nelson, and Thomas modeling of the fix-bed continuous column adsorption of amoxicillin onto silver nanoparticle-maize leaf composite. *Appl Water Sci*. 2022;12:94. doi: 10.1007/s13201-022-01624-4
- Cardoso B, Mestre AS, Carvalho AP, Pires J. Activated carbon derived from cork powder waste by KOH activation: Preparation, characterization, and VOCs adsorption. *Ind Eng Chem Res*. 2008;47:5841-5846. doi: 10.1021/ie800338s

13. Ochai-Ejeh FO, Madito MJ, Momodu DY, Khaleed AA, Olaniyan O, Manyala N. High performance hybrid supercapacitor device based on cobalt manganese layered double hydroxide and activated carbon derived from cork (*Quercus suber*). *Electrochim Acta*. 2017;252:41-54.
doi: 10.1016/j.electacta.2017.08.163
14. Thitame PV, Shukla SR. Porosity development of activated carbons prepared from wild almond shells and coir pith using phosphoric acid. *Chem Eng Commun*. 2015;203:791-800.
doi: 10.1080/00986445.2015.1104503
15. Nasrullah A, Saad B, Bhat AH, *et al*. Mangosteen peel waste as a sustainable precursor for high surface area mesoporous activated carbon: Characterization and application for methylene blue removal. *J Clean Prod*. 2019;211:1190-1200.
doi: 10.1016/j.jclepro.2018.11.094
16. Foo KY, Hameed BH. Utilization of rice husks as a feedstock for preparation of activated carbon by microwave induced KOH and K₂CO₃ activation. *Bioresour Technol*. 2011;102:9814-9817.
doi: 10.1016/j.biortech.2011.07.102
17. Sun D, Zhang Z, Wang M, Wu Y. Adsorption of reactive dyes on activated carbon developed from *Enteromorpha prolifera*. *Am J Anal Chem*. 2013;4:17-26.
doi: 10.4236/msce.2018.64006
18. Silva TL, Ronix A, Pezoti O, *et al*. Mesoporous activated carbon from industrial laundry sewage sludge: Adsorption studies of reactive dye Remazol Brilliant Blue R. *Chem Eng J*. 2016;303:467-476.
doi: 10.1016/j.cej.2016.06.009